Enormous Enhancement of van der Waals Forces between Small Silver Particles

Heinz Burtscher

Laboratory for Solid State Physics, Eidgenossische Technische Hochschule, CH-8093 Zürich, Switzerland

and

Andreas Schmidt-Ott

Atmospheric Physics and Laboratory for Solid State Physics, Eidgenossische Technische Hochschule, CH-8093 Zürich, Switzerland

Dispersion forces enhance the coagulation rate of small particles in a gas. Measurements of coagulation rates on ultrafine Ag and C particles with radii of 3–16 nm were performed. The results obtained with C particles almost agree with the expectations based on bulk electronic properties. However, Ag particles 14 nm in radius exhibit a very large coagulation rate. It points to an enhancement of the dispersion forces of at least a factor of 10^4.

PACS numbers: 61.50.Lt, 82.70.Rr

Optical properties of ultrafine particles have attracted considerable interest. Experiments and calculations pointing to very large deviations of the dielectric properties from bulk values have been reported by several authors.[1-4] The purpose of this Letter is to report on an enhancement of van der Waals or dispersion forces between fine Ag particles with radii around 14 nm. The results are obtained by measuring the coagulation or agglomeration rate of Ag and C particles in gas suspension. Enhanced coagulation rates have been observed before[5,6] but have not been ascribed to enhanced dispersion forces. Here a relationship between the coagulation rate and the dispersion potential is derived and applied to experimental results.

It can be shown that every collision of particles larger than a few nanometers leads to coagulation, since dispersion forces guarantee sticking.[7] The Brownian coagulation of particles of a certain size is described by[8]

$$dZ/dt = -\tfrac{1}{2}KZ^2, \tag{1}$$

where Z is the particle number concentration and K the coagulation coefficient, which depends on the particle size. For the treatment of aerosols containing a size distribution of particles, the size spectrum is divided into size intervals i with mean radii $\bar{R}_i$, where $\bar{R}_{i+1} = 2\bar{R}_i$. Furthermore, the following assumptions are made: (i) On average, size interval i gains a particle by coagulation of m particles in size interval $i-1$. (ii) A particle is lost to size interval i by coagulation with a particle in interval j $(j \geq i)$. If $j > i$, the concentration in interval j is not changed by this process. (iii) The coagulation coefficient is constant within each interval. With these assumptions the concentration in interval i is described by

$$2\frac{dZ_i}{dt} = \frac{1}{m} K_{i-1,i-1} Z_{i-1}{}^2 - Z_i \sum_{j=i}^{\infty} K_{i,j} Z_j, \tag{2}$$

where K_{ij} is the coagulation coefficient for coagulation of a particle in interval i with one in interval j.

In the experiment, the coagulation is monitored by measuring the concentrations Z_i as a function of time. The particles are produced in a continuous N_2 flow (2 L/min) either by electrode sputtering in a spark discharge between C or Ag electrodes or by electrically heating an Ag wire. Electron micrographs show that the particles are essentially spherical and only partly agglomerated. The aerosol is then passed through an electrostatic filter where all charged particles are removed and diluted with particle-free air (~ 25 l/min). It is then filled into a conductive plastic bag. Subsequently, some of the aerosol is continuously removed for size and concentration analysis. The particle concentration before coagulation in the bag is controlled by dilution such that the diffusion loss of particles in the bag is negligible compared to coagulation.

Size and concentration analysis is done by two different methods: The first one is based on a particle mobility analysis in a commercially available electrostatic aerosol analyzer (EAA).[9,10] The EAA yields the particle concentration in size intervals i with average radii $\bar{R}_{i+1} = 2\bar{R}_i$. It is sensitive to particles with radii > 3.4 nm. Alternatively, a method based on photoelectron emission from the particles by irradiation of an aero-

sol with ultraviolet light is applied. In air, the photoelectrons form negative small ions. These ions and the positively charged particles cause a conductivity Σ [aerosol photoconductivity[1] (APC)] which is measured by an ac method.[11] The time dependence $\Sigma(t)$ when the aerosol is exposed to the light and after removal of the light is governed by the photoelectron emission rate and the diffusion of small ions and particles to the walls of the confinement. Under the assumption of a narrow particle-size distribution, $\Sigma(t)$ yields the mean particle size and concentration.[1] Because of the high photothreshold of C, this method can only be applied to the Ag aerosol.

All measurements are done at room temperature. First Ag and C aerosols are prepared by the sputtering method. Particles occur in three size intervals. Figure 1 shows the measured $Z_i(t)$ for the Ag aerosol. The coagulation coefficients K_{ij} as well as m are evaluated by computer fit of Eq. (2) to the measured $Z_i(t)$, using the simplifying assumption $K_{ii} = K_{i,i+1}$. Furthermore, K_{13} and terms with i or $j \geq 4$ are set equal to 0 because the corresponding concentrations are negligible or zero. The curves in Fig. 1 represent the fit which is optimal for $m = 5$. Table I shows the obtained coagulation coefficients. The large range of uncertainty for the coefficients arises from the following sources of error:
(i) A systematic error in the absolute EAA concentration determination is possible, especially for the smallest size interval.[9,10] The results shown represent the worst case when assuming errors of -50% and $+100\%$ for interval 1 and

$\pm 15\%$ for intervals 2 and 3. (ii) The relative standard deviation of the measured values from the fitted ones is 9%. The statistical error is thus of minor importance compared to the assumed systematic error. The reason for the statistical fluctuations is that the spark aerosol source was not completely steady and the coagulating aerosol was therefore slightly inhomogeneous.

Besides the measurements for Ag and C described above, APC and EAA are applied to similar aerosols of ultrafine Ag particles ($\bar{R} \approx 3.5$ nm) produced by the wire method. The size distribution of these particles before coagulation is so narrow that only the first EAA size interval responds to them. Therefore, these measurements yield values for K_{11} only (see Table I). The fair agreement between the values gained by APC and EAA supports the EAA method.

The resulting coagulation rate for Ag is very large compared to the one obtained for C. A diffusion battery placed into the aerosol stream before the EAA, modifies the size spectra for Ag and C in the same way, confirming identical diffusion behavior. Therefore, the discrepancies in coagulation must be ascribed to attractive forces. Since the particles are electrically neutral, we ascribe them to dispersion forces. A calculation of aerosol coagulation coefficients involving dispersion potentials on the basis of bulk dielectric data has been done by Marlow.[12] The enhancements K/K_0 (where K_0 is the value for force-free coagulation according to a theory by Fuchs[13]) which Marlow obtains are not far from
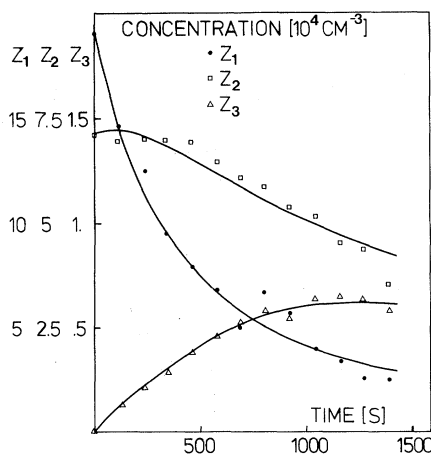

FIG. 1. Concentration of Ag particles in the three EAA size classes versus time: Z_1, 2.8–5 nm radius; Z_2, 5–8.3 nm radius; Z_3, 8.3–16 nm radius.

TABLE I. Summary of results. Calculated values by Marlow; particles generated by wire (w) and sputtering (s).

	Mean radius (nm)	$10^8 K_{ii}$ [s^{-1} cm^3]	K_{ii}/K_0	Method
Ag (w)	3.5	$K_{11} \approx 1.35$	≈ 6.8	APC
	3.5	$K_{11} \approx 0.3-3.6$	1.5–18	EAA
Ag (s)	3.5	$K_{11} = 1.2-3.4$	6–17	
	7	$K_{22} = 1.1-2.7$	5.5–13	EAA
	14	$K_{33} = 6-57$	30–285	
C (s)	3.5	$K_{11} = 0.12-1.6$	0.6–8	
	7	$K_{22} = 1.2-1.6$	6–8	EAA
	14	$K_{33} = 0.27-0.6$	1.4–3	
Ag	1		4.86	
	100		1.25	Calculated
C	1		4.0	
	100		1.16	

agreement with the coagulation rates observed for C but they fail to explain the rapid coagulation of Ag particles in the 14-nm interval. This leads to the conclusion that van der Waals forces between these silver particles are much larger than expected from calculations using bulk dielectric data.

An estimate for this enhancement is derived following the ideas of Schmidt-Ott and Burtscher.[14] Langbein[15] has shown that the nonretarded dispersion potential between spheres is

$$\varphi < \varphi_L$$
$$= -A\left[\frac{R^2}{2}\left(\frac{1}{r^2 - 4R^2} + \frac{1}{r^2}\right) + \frac{1}{4}\ln\frac{r^2 - 4R^2}{r^2}\right], \quad (3)$$

where φ_L corresponds to the macroscopic theory of Lifschitz. In (3), A is the material-dependent term; the rest contains information about geometry only. As an upper limit, (3) is also valid when retardation is taken into account. According to the Lifschitz theory, A is defined by $A = \hbar\bar{\omega}/2\pi$, where $\hbar\bar{\omega}$ is the Lifschitz–van der Waals constant. This definition is not necessarily applicable in the enhanced small-particle case. The continuum theory for coagulation yields the Smoluchowski formula[8]

$$K = 16\pi D(R)R_{eff}, \quad (4)$$

with $D(R)$ denoting the particle diffusion constant which is given by the Stokes-Cunningham equation.[8] For force-free coagulation the effective particle-collision radius $R_{eff} = R$, and if forces between the particles are accounted for,

$$R_{eff} = \frac{1}{2}\left[\int_{2R}^{\infty}\frac{1}{r^2}\exp\left(\frac{\varphi(r)}{kT}\right)dr\right]^{-1}, \quad (5)$$

where $\varphi(r)$ is the corresponding potential as a function of the distance of particle centers. Equations (4) and (5) are rigorous in the continuum range, i.e., on a scale larger than the apparent particle free path between collisions with the gas molecules. The validity range is commonly given in terms of λ_g/R, λ_g being the gas-molecule free path. We infer from Ref. 8 that the error in K is less than a few percent if $\lambda_g/R < 2.5$. For collisions aided by attractive forces the effective radius R_{eff}, representing the distance at which the particles are trapped, is relevant rather than the particle radius. With $\lambda_g = 60$ nm (air at normal conditions) we obtain the condition

$$R_{eff} > 24 \text{ nm.} \quad (6)$$

It must be noted that, according to (3), $\varphi(r)$ falls very rapidly. This means that A is extremely sensitive to R_{eff} or K but not to the temperature T. The results are the following:

(i) The immense difference between the coagulation rates measured for Ag and C under identical conditions (EAA) implies an enormous K enhancement for Ag particles around 14 nm in radius, regardless of the absolute precision of the EAA.

(ii) A lower limit for the constant A(particle) can be calculated from (3)–(5) for Ag particles of $R = 14$ nm, since for them condition (6) is well fulfilled ($R_{eff} > 120$ nm). With A(bulk) $= (10.4$ eV$)/2\pi$,[16] the enhancement $\alpha = A$(particle)$/A$(bulk) $> 10^4$ for these particles.

(iii) The coagulation enhancement factor K/K_0 of Ag particles increases drastically for increasing radius in the size range investigated. Since K/K_0 must approach unity for large radii this implies a relative maximum of $K(R)/K_0$, and thus also for $\alpha(R)$.

Dispersion forces between small Ag particles seem to exhibit some resonant behavior that does not occur in the extended metal. The relative maximum of $\alpha(R)$ indicates that the resonance occurs for a certain particle size. Entirely different optical properties of small particles compared to the bulk metal have been reported before, for instance an infrared absorption enhancement by a factor of 200, occurring quite abruptly at $R = 10$ nm.[3] For surface-enhanced Raman scattering (SERS) from adsorbates on rough metal surfaces[2] or isolated small particles,[17] enhancements of 10^6 have been measured and calculated, respectively. Numerous approaches to explanations of SERS have been proposed.[2] For photoemission from Ag particles ($R = 25$ nm) a quantum yield enhancement of a factor of 100 occurred, due to enhanced absorption.[1] Calculations by Penn and Rendell[4] show that the spatial variation of the photon field at the metal surface associated with the excitation of electron-hole pairs in small particles results in an enhanced absorption. For small spheres, electron-hole excitation can dominate the absorption, and thus may be responsible for the size effects mentioned.

[1]A. Schmidt-Ott, P. Schurtenberger, and H. C. Siegmann, Phys. Rev. Lett. 45, 1284 (1980).

[2]E. Burstein, C. Y. Chen, and S. Lundquist, in Light

Scattering in Solids, edited by J. L. Birman, H. Z. Cummins, and K. K. Rebane (Plenum, New York, 1979).

[3]D. B. Tanner, A. J. Sievers, and R. A. Buhrman, Phys. Rev. B 11, 1330 (1975).

[4]D. R. Penn, R. W. Rendell, Phys. Rev. Lett. 47, 1067 (1981).

[5]J. Stockham, Microscope 15, 106 (1966).

[6]S. C. Graham and J. B. Homer, Disc. Faraday Symp. 7, 85 (1973).

[7]S. Twomey, *Atmospheric Aerosols* (Elsevier, New York, 1977).

[8]G. M. Hidy and J. R. Brock, *The Dynamics of Aerocolloidal Systems* (Pergamon, New York, 1970).

[9]K. T. Whitby and B. K. Cantrell, in *Aerosol Measurement*, edited by D. A. Lundgren *et al.* (University

Presses of Florida, Gainesville, 1979).

[10]*Aerosol Measurement*, edited by D. A. Lundgren *et al.* (University Presses of Florida, Gainesville, 1979), pt. III.

[11]A. Schmidt-Ott and H. C. Siegmann, Appl. Phys. Lett. 32, 710 (1978).

[12]W. H. Marlow, Surf. Sci. 106, 529 (1980).

[13]N. A. Fuchs, *The Mechanics of Aerosols* (Pergamon, New York, 1964).

[14]A. Schmidt-Ott and H. Burtscher, to be published.

[15]D. Langbein, J. Phys. Chem. Solids 32, 1657 (1971).

[16]H. Krupp, W. Schnabel, and G. Walter, J. Coll. Interface Sci. 39, 421 (1972).

[17]M. Kerker, D. S. Wang, and H. Chew, Appl. Opt. 19, 3373 (1980).

Critical Cone in Phonon-Induced Desorption of Helium

Peter Taborek

Bell Laboratories, Murray Hill, New Jersey 07974

A flash desorption technique is used to show that helium atoms desorbing from a hot surface are emitted within a narrow cone about the normal direction. The emission angle and the energy of the atoms are highly correlated, which results in a "rainbow" in the desorption spectrum. These effects are discussed in terms of single-particle conservation conditions for energy and momentum transfer between phonons and atoms.

PACS numbers: 68.45.Da

Phonons in a solid substrate can interact with atoms on a surface by causing displacements which modulate the local surface potential. An adsorbed atom initially in a bound state can be desorbed by this perturbation. A quantum theory of this process of phonon-induced desorption was first considered by Lennard-Jones and co-workers,[1] but several more sophisticated treatments have recently appeared.[2-6] Using these theories, one can express the momentum distribution of the desorbed atoms in terms of a perturbation series expansion involving the phonon distribution and the surface-adatom interaction. First-order perturbation theory yields a value for the probability of a 1-phonon desorption process of the form $|M|^2/\omega$, where ω is the phonon frequency and $|M|^2$ is a squared matrix element which depends only on the initial and final states of the atom; the probability of multiphonon desorption processes is related to higher orders of the perturbation which are much more complicated and difficult to compute.[6]

Although the 1-phonon approximation has been useful in explaining atomic beam scattering results,[7] it is difficult to test the simple desorption theories decisively using only the available data on the desorption rate and the energy distribution. In contrast, the complete three-dimensional (3D) distribution of the atomic momentum provides a much more sensitive probe of the desorption process. Previous measurements of the angular distribution of desorption[8,9] have involved systems at such high temperatures and with such strong adatom-substrate interactions that the 1-phonon perturbation theories are not applicable. Helium, with a binding energy an order of magnitude smaller than most other adsorbates, provides a good test case for theories based on the weak coupling approximation which suggest that at low temperatures 1-phonon processes should be the dominant desorption mechanism. Quantitative comparison with the published theories is difficult, however, because of uncertainties in the parameters which determine $|M|^2$; moreover, the most detailed calculations assume that the adatom is localized to a site on the substrate, which is probably not an appropriate model for helium on a metallic surface.[10] Despite these